Controllability limit of edge dynamics in complex networks

Shao-Peng Pang,[1,*] Wen-Xu Wang,[2,3] and Fei Hao[4]

[1]*School of Electrical Engineering and Automation, Qilu University of Technology (Shandong Academy of Science), Jinan, Shandong Province 250353, China*

[2]*State Key Laboratory of Cognitive Neuroscience and Learning IDG/McGovern Institute for Brain & Research, Beijing Normal University, Beijing 100875, China*

[3]*School of Systems Science, Beijing Normal University, Beijing 100875, China*

[4]*The Seventh Research Division, School of Automation Science and Electrical Engineering, Beihang University, Beijing 100191, China*

(Received 14 April 2019; published 27 August 2019)

Edge dynamics is relevant to various real-world systems with complex network topological features. An edge dynamical system is controllable if it can be driven from any initial state to any desired state in finite time with appropriate control inputs. Here a framework is proposed to study the impact of correlation between in- and out-degrees on controlling the edge dynamics in complex networks. We use the maximum matching and direct acquisition methods to determine the controllability limit, i.e., the limit of acceptable change of the edge controllability by adjusting the degree correlation only. Applying the framework to plenty complex networks, we find that the controllability limits are ubiquitous in model and real networks. Arbitrary edge controllability in between the limits can be achieved by properly adjusting the degree correlation. Moreover, a nonsmooth phenomenon occurs in the upper limits, and exponential and power-law scaling behaviors are widespread in the approach or separation speed between the upper and lower limits.

DOI: 10.1103/PhysRevE.100.022318

I. INTRODUCTION

Networked structures are common in most social, physical, biological, and technological systems [1–3]. How to control complex networks is one of the most challenging problems in modern network science [4–6]. Liu *et al.* [7] made a breakthrough by developing structural control theory for complex networks and offered efficient tools based on the maximum matching to characterize the controllability of directed networks. Much interest has been stimulated toward exploring controllability properties of complex networks [8–19].

By far most studies of network controllability are carried out based on nodal dynamics, in which variables are defined on nodes and interactions occur among the neighboring nodes. However, the behavior of edge dynamics is also very important in network science. A pioneering work to address the edge controllability was proposed by Nepusz *et al.* [20]. They introduced switchboard dynamics to describe the edge dynamics in complex networks and developed structural edge controllability. Then we expanded the switchboard dynamics to the generalized switchboard dynamics (GSBD) [21] to characterize a dynamical process on the edges of directed and undirected networks with arbitrary interaction strengths among edges. Many findings of controllability properties of the GSBD significantly differ from that of nodal dynamics and structural edge controllability. Representative discovery is that the interaction strength plays a more important role in the edge controllability than network structure. Despite the interesting findings, the simulation and analytical results of the edge controllability in Ref. [21] are performed by assuming that in- and out-degrees are uncorrelated in complex networks. Some studies already suggest a correlation between in- and out-degrees in real networks [22,23]. It is unreasonable to assume that such degree correlation has no influence on edge controllability. We refer to correlation between in- and out-degrees as degree correlation in the remainder of this paper for simplicity.

In this paper, we focus on the degree correlation on edge controllability. The edge controllability is measured by the minimum numbers of driver nodes and driven edges. A framework based on the maximum matching is proposed to determine the limit of acceptable change of the edge controllability by adjusting the degree correlation only. We use this framework to uncover a number of phenomena associated uniquely with the edge controllability. Specifically, the degree correlation plays an important role in edge controllability. There exist universal lower and upper limits of edge controllability for model and real networks. A vast range is existed between the limits, especially for networks with structural switching matrices. Arbitrary edge controllability in between the limits can be achieved by properly adjusting the degree correlation. A nonsmooth phenomenon occurs in the upper limits of part model networks. Exponential and power-law scaling behaviors are widespread in the approach or separation speed between the upper and lower limits of model networks. For all the results concerning nonsmooth, exponential and power-law scaling behaviors, we provide the analytic formula and results from extensive numerical tests. In summary, our findings indicate that it is imperative to consider the degree correlation to offer a better understanding of the edge controllability.

*pang_shao_peng@163.com

II. CONTROLLING EDGE DYNAMICS

The GSBD [21] provides a general characterization of dynamics occurring on edges of a directed network $G(V, E)$. Let $\mathbf{y}_v^-$ and $\mathbf{y}_v^+$ denote the state vectors comprised of the states of the incoming and outgoing edges of node v, respectively. The state vector $\mathbf{y}_v^+$ can be influenced by the state vector $\mathbf{y}_v^-$, the vector of the damping terms $\boldsymbol{\tau}_v$ and the external input vector $\mathbf{u}_v$. So the equation governing the edge dynamics is

$$\dot{\mathbf{y}}_v^+ = S_v \mathbf{y}_v^- - \boldsymbol{\tau}_v \otimes \mathbf{y}_v^+ + \sigma_v \mathbf{u}_v, \tag{1}$$

where $S_v \in \mathbb{R}^{k_v^+ \times k_v^-}$ is the general switching matrix with row number equaling the out-degree k_v^+ and column number equaling the in-degree k_v^- of node v. $\otimes$ denotes the entrywise product of the two vectors of the same size. σ_v is 1 if node v is a driver node and 0 otherwise. Note that the elements in S_v capture the interaction strengths among edges. In the structural edge controllability [20], S_v must be a structural matrix, in which all nonzero elements are independent free parameters. Instead, the GSBD releases the restriction of S_v, in which the elements could be arbitrary fixed values (including 0). A correspondence between the GSBD and the linear time-invariant dynamical system can be established by reformulating Eq. (1) in terms of x_i of the edges, yielding

$$\dot{\mathbf{x}} = (W - T)\mathbf{x} + H\mathbf{u}, \tag{2}$$

where $W \in \mathbb{R}^{M \times M}$ is the transpose matrix of the adjacency matrix of the line graph $L(G)$ of G, in which w_{ij} is nonzero if and only if the head of edge j is the tail of edge i. $T \in \mathbb{R}^{M \times M}$ is a diagonal matrix composed of the damping terms of each edge. $H \in \mathbb{R}^{M \times M}$ is a diagonal matrix where the ith diagonal element is σ_v if node v is the tail of edge i. Note that for the edge dynamics in undirected networks, the GSBD can be defined by splitting each undirected edge into two directed edges with opposite directions. Each undirected edge is denoted by a couple of state variables (x_i, x_i') corresponding to its two directed edges. For the whole network, the dynamical process can be still described by Eq. (2), but matrices W, T, and H belong to $\mathbb{R}^{2M \times 2M}$.

One key result in Ref. [21] is that the minimum number of driver nodes can be determined by selecting the nodes without full row-rank switching matrix ($\mathrm{rank}(S_v) < k_v^+$) and one arbitrary node from each full rank component (the switching matrices of all nodes in a connected component are square matrices with full rank). Each driver node must control $k_v^+ - \mathrm{rank}(S_v)$ of its outgoing edges, and the selected nodes in each full rank component must control one of its outgoing edges. Moreover, there exist upper and lower bounds of the numbers of driver nodes and driven edges required to maintain full control, which are determined by the interaction strengths. The upper and lower bounds are reached if S_v of each node is an unweighted matrix (all elements are one) and a structural matrix, respectively.

Despite the interesting findings, the simulation and analytical results of the edge controllability in Ref. [21] are performed by assuming that in- and out-degrees of each node are uncorrelated in complex networks. So we will be interested in the effect of the degree correlation on the edge controllability in this paper.

III. CONTROLLABILITY LIMITS

The edge controllability is measured by the minimum number N_D of driver nodes and the minimum number M_D of driven edges required to maintain full control [20,21]. The criterion for discerning driver nodes and driven edges in Ref. [21] indicates that the edge controllability is influenced by the interaction strength. In order to exclude the influence from the interaction strength, only the upper and lower bounds of edge controllability are considered in this paper. Specifically, for a directed network with unweighted switching matrices corresponding to the upper bound or with structural switching matrices corresponding to the lower bound, we analyze the limits of acceptable change of its N_D and M_D by adjusting the degree correlation only. The upper and lower limits of N_D and M_D are simply referred to as controllability limits.

For a directed network with structural switching matrices, a node v can contribute rank $\min(k_v^-, k_v^+)$. So the node with $k_v^+ > k_v^-$ must be a driver node. Each driver node must control $k_v^+ - k_v^-$ of its outgoing edges. The dependence of driver node and driven edge on local structures allows us to determine the controllability limits by the maximum matching. For the upper limit of N_D, the maximum matching is used to find out the maximum possible number of divergent nodes constituted by the in- and out-degree sequences of the network. Specifically, an undirected bipartite graph H with $2N$ nodes is generated by the in-degree sequence $K_{\mathrm{in}} = \{k_1^-, k_2^-, \ldots, k_N^-\}$ and the out-degree sequence $K_{\mathrm{out}} = \{k_1^+, k_2^+, \ldots, k_N^+\}$ of the network. As shown in Fig. 1(a), i from in-degree sequence and j from out-degree sequence are connected if $k_i^- < k_j^+$. Each edge in H corresponds to a potential driver node in the generated network. So the upper limit of N_D can be given by

$$N_D^U = \max(1, |M_H|), \tag{3}$$

where $|M_H|$ is the number of edges in the maximum matching of H. For the lower limit of N_D, as shown in Fig. 1(b), an undirected bipartite graph $\overline{H}$ is generated by connecting i from in-degree sequence and j from out-degree sequence if $k_i^- \geqslant k_j^+$. Each edge in $\overline{H}$ corresponds to a potential nondriver node in the generated network. So the lower limit of N_D can be described by

$$N_D^L = \max(1, N - |M_{\overline{H}}|), \tag{4}$$

where $|M_{\overline{H}}|$ is the number of edges in the maximum matching of $\overline{H}$. For the upper limit of M_D, as shown in Fig. 1(c), a weighted bipartite graph H^* is generated by assigning the weight $k_j^+ - k_i^-$ to each edge in H. An edge weight corresponds to the number of outgoing edges controlled by a potential driver node in the generated network. So the upper limit of M_D can be given by

$$M_D^U = \max(1, |M_{H^*}|), \tag{5}$$

where $|M_{H^*}|$ is the sum of edge weights in the weighted maximum matching of H^*. For the lower limit of M_D, as shown in Fig. 1(d), a weighted bipartite graph $\overline{H^*}$ is generated by connecting arbitrary two nodes from in- and out-degree sequences. The edge weight is $k_i^- - k_j^+$ if the edge satisfies $k_i^- < k_j^+$ and 0 otherwise. The absolute value of an edge weight corresponds to the number of outgoing edges controlled by a potential driver node in the generated network. So the lower limit of M_D can be described by

$$M_D^L = \max(1, |M_{\overline{H^*}}|), \tag{6}$$

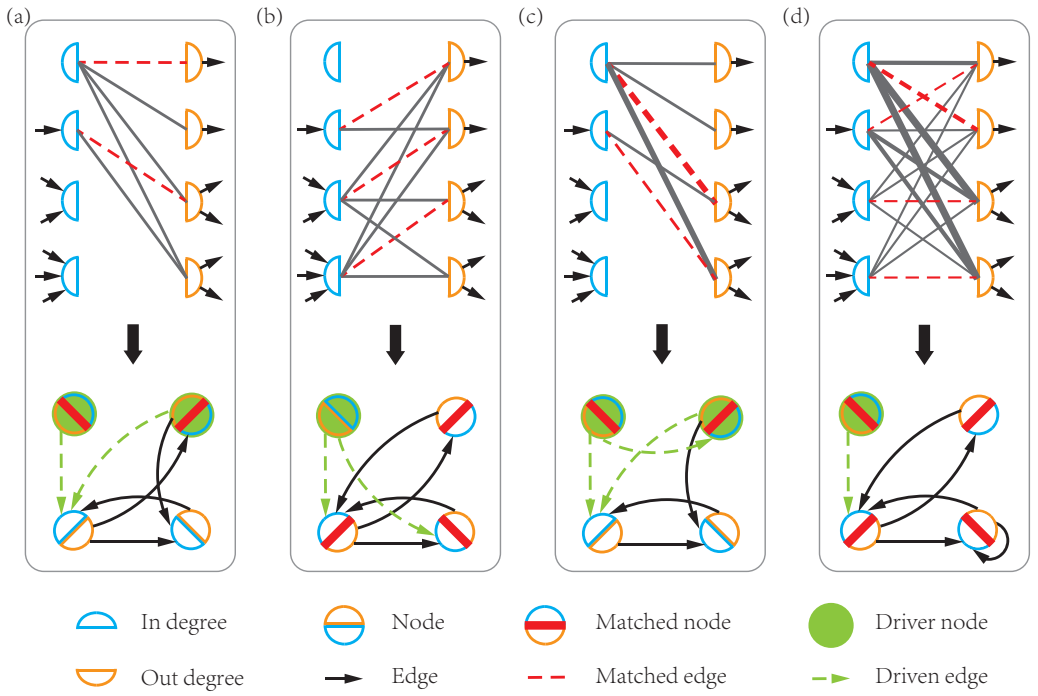

FIG. 1. Controllability limits. (a) Upper limit of N_D. An undirected bipartite graph H generated by the in-degree sequence $K_{\text{in}} = \{0, 1, 2, 3\}$ and the out-degree sequence $K_{\text{out}} = \{1, 1, 2, 2\}$, where node i from the in-degree sequence and node j from the out-degree sequence are connected if $k_i^- < k_j^+$. Its generated network in has $N_D^U = 2$. (b) Lower limit of N_D. An undirected bipartite graph $\overline{H}$ generated by connecting i from the in-degree sequence and j from the out-degree sequence if $k_i^- \geqslant k_j^+$. Its generated network in has $N_D^L = 1$. (c) Upper limit of M_D. A weighted bipartite graph H^* is generated by assigning the value $k_j^+ - k_i^-$ to each edge in H. Its generated network in has $M_D^U = 3$. (d) Lower limit of M_D. A weighted bipartite graph $\overline{H^*}$ is generated by connecting arbitrary two nodes, and assigning the value $k_i^- - k_j^+$ to the edges satisfied $k_i^- < k_j^+$, and zero for other edges. Its generated network in has $M_D^L = 1$. Note that the matching nodes in the generated networks are from the matched edges in the maximum matching, and other nodes are randomly generated.

where $|M_{\overline{H^*}}|$ is the absolute values of the sum of edge weights in the weighted maximum matching of $\overline{H^*}$.

For a directed network with unweighted switching matrices, a node v with $k_v^+ > 0$ and $k_v^- > 0$ can only contribute rank one. So the node with $k_v^+ > 1$ or the node with $k_v^+ = 1$ and $k_v^- = 0$ must be a driver node. Each driver node with $k_v^+ > 0$ and $k_v^- > 0$ must control $k_v^+ - 1$ of its outgoing edges, and each driver node with $k_v^+ > 0$ and $k_v^- = 0$ must control all of its outgoing edges. The dependence of driver node and driven edge on local structures enables us to directly determine the controllability limits. Detailed results are shown in Table I.

In summary, the controllability limits of any directed network can be calculated by means of maximum matching or direct acquisition. Note that we do not consider the undirected network because all nodes in the undirected network are balanced ($k_v^- = k_v^+$). In addition, the full rank component is infrequent in directed networks. It have little influence to N_D and M_D [20,21]. We thus neglect the possible presence of the full rank component when analyze the controllability limits.

IV. CONTROLLABILITY LIMITS IN MODEL NETWORKS

We employ the model and real networks to substantiate the controllability limits. Figure 2 shows their average degree $\langle k \rangle$ dependence for Erdős-Rényi (ER) random network [24] and exponential (EX) network, and power-law exponent γ

TABLE I. Controllability limits. The upper and lower limits of N_D and M_D. The number of nodes under some conditions is defined as $N(*)$ with the conditions in its subscript.

	Unweighted switching matrix	Structural switching matrix
N_D^U	$N_{(k_v^+>1)} + \min(N_{(k_v^+=1)}, N_{(k_v^-=0)})$	$\max(1, \lvert M_H \rvert)$
N_D^L	$\begin{cases} N_{(k_v^+>1)} & \text{if } N_{(k_v^+=1)} \leqslant N_{(k_v^-=0)} \\ N_{(k_v^+>1)} + N_{(k_v^+=1)} - N_{(k_v^-=0)} & \text{if } N_{(k_v^+=1)} > N_{(k_v^-=0)} \end{cases}$	$\max(1, N - \lvert M_{\overline{H}} \rvert)$
M_D^U	$\begin{cases} M & \text{if } N_{(k_v^+>0)} \leqslant N_{(k_v^-=0)} \\ M - N_{(k_v^+>0)} + N_{(k_v^-=0)} & \text{if } N_{(k_v^+>0)} > N_{(k_v^-=0)} \end{cases}$	$\max(1, \lvert M_{H^*} \rvert)$
M_D^L	$M - \min(N_{(k_v^+>0)}, N_{(k_v^-=0)})$	$\max(1, \lvert M_{\overline{H^*}} \rvert)$

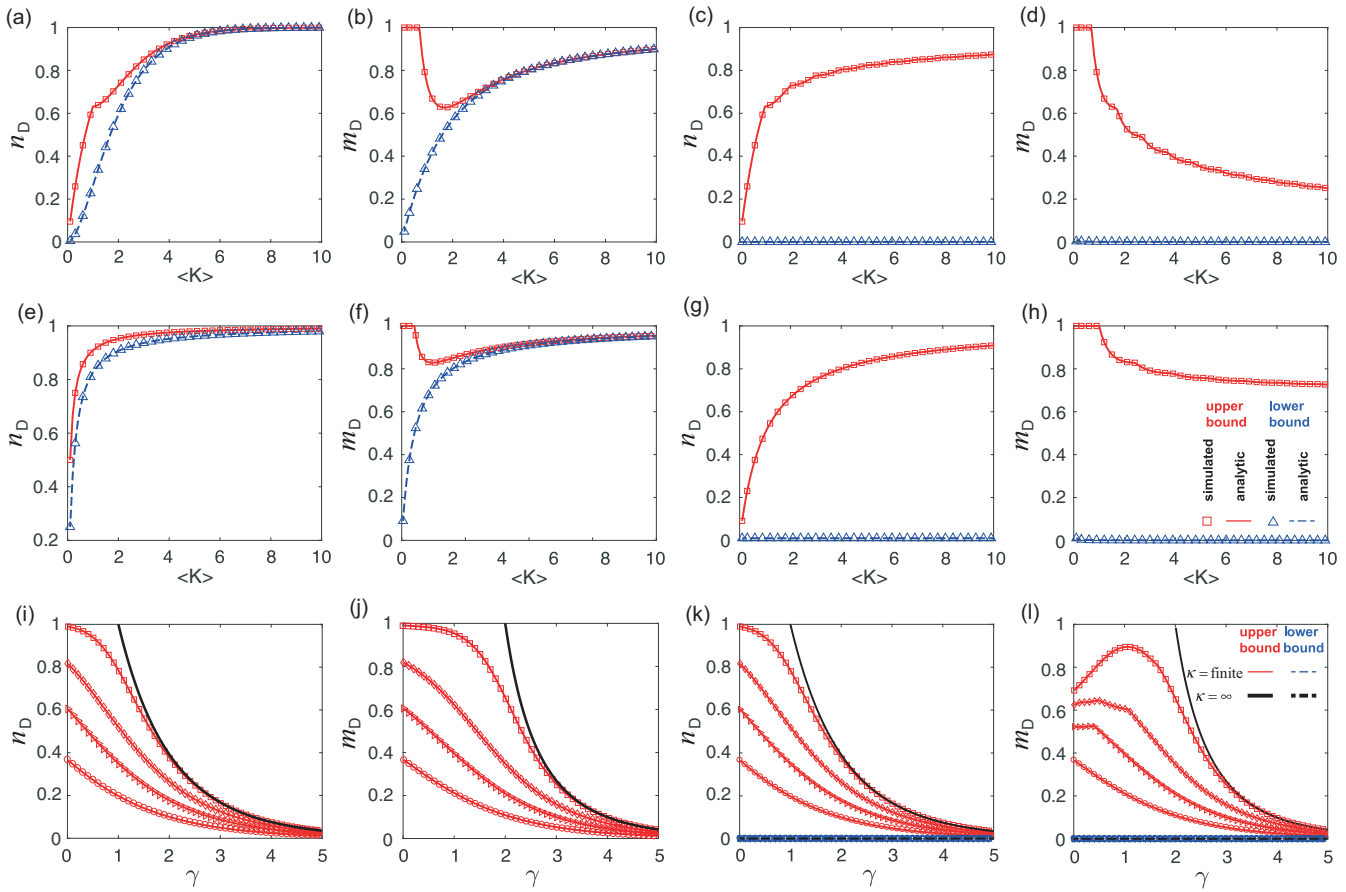

FIG. 2. Controllability limits in model networks. The upper and lower limits of driver nodes and driven edges in [(a)–(d)] ER networks and [(e)–(h)] EX networks as the function of the average degree $\langle k \rangle$ and in [(i)–(l)] SF networks as the function of the power-law exponent γ and the exponential cutoff parameter κ. The exponential cutoff parameter for the red full lines in (j) and (l) is, from top to bottom, $\kappa = 1, 2, 5, 100$, and reverse order for others. The controllability limits of model networks with unweighted switching matrices are shown in (a), (b), (e), (f), (i), and (j) and with structural switching matrices are shown in (c), (d), (g), (h), (k), and (l). How to generate model networks are presented in Appendix A.

dependence for scale-free (SF) network [25]. An important observation is that the upper and lower limits of n_D and m_D hold for all kinds of model networks. Any values of n_D and m_D in between the limits are achievable by properly adjusting the degree correlation. This demonstrates that the degree correlation plays an important role in the edge controllability. Another notable result is that, the degree correlation has a bigger effect on n_D and m_D in networks with structural switching matrices, in which the range between the upper and lower limits is very large. Conversely, the impact of the degree correlation is very limited in networks with unweighted switching matrices. This shows that the edge controllability of networks with structural switching matrices is more susceptible to the degree correlation. Note that the upper and lower limits in SF networks with unweighted switching matrices [see Fig. 2(i) and 2(j)] are the same because $P_0^{\text{in}} = P_0^{\text{out}} = 0$ in SF model networks, where P_k^{in} and P_k^{out} are the in-degree distribution and the out-distribution distribution, respectively. The detailed procedures for deriving the analytical results are presented in Appendix B. As shown in Fig. 2, the analytical results are in fairly good agreement with numerical simulations.

A nonsmooth phenomenon occurs in the upper limit of n_D of ER networks [see Fig. 2(c)], and the upper limit of m_D of the ER, EX, and SF networks [see Figs. 2(d), 2(h) and 2(l)]. In ER networks, both in- and out-degrees follow the Poisson distribution, which is $P_k^{\text{in}} = P_k^{\text{out}} = \langle k \rangle^k e^{-\langle k \rangle}/k!$, where $\langle k \rangle$ is the average degree. The Poisson distribution is a unimodal distribution. The degree of its peak is a step function that increases with $\langle k \rangle$, i.e., $k_{\text{peak}} = \lfloor \langle k \rangle \rfloor$, where $\lfloor \langle k \rangle \rfloor$ is the largest integer not greater than $\langle k \rangle$. The k_{peak} is the origin of the nonsmooth phenomenon in the upper limit of n_D in ER networks. In contrast, in ER, EX and SF networks, the nonsmooth phenomenon in the upper limit of m_D stems from the median k_{mid} of the ordered degree sequence, where k_{mid} is also a step function that increases with $\langle k \rangle$ in ER and EX networks, and with γ in SF netwotks. See Appendix C for details.

The simulation results in Fig. 2 show that the upper and lower limits approach or separate from each other as $\langle k \rangle$ and γ increase. This inspired us to study the approach or separation speed between the upper and lower limits, where the speed is defined as $(n_D^U - n_D^L)'$ and $(m_D^U - m_D^L)'$. We find that a speed scaling law is ubiquitous in model networks. Specifically, as shown in Fig. 3, a exponential scaling behavior exists in ER networks with unweighted switching matrices and SF networks, and a power-law scaling behavior exists

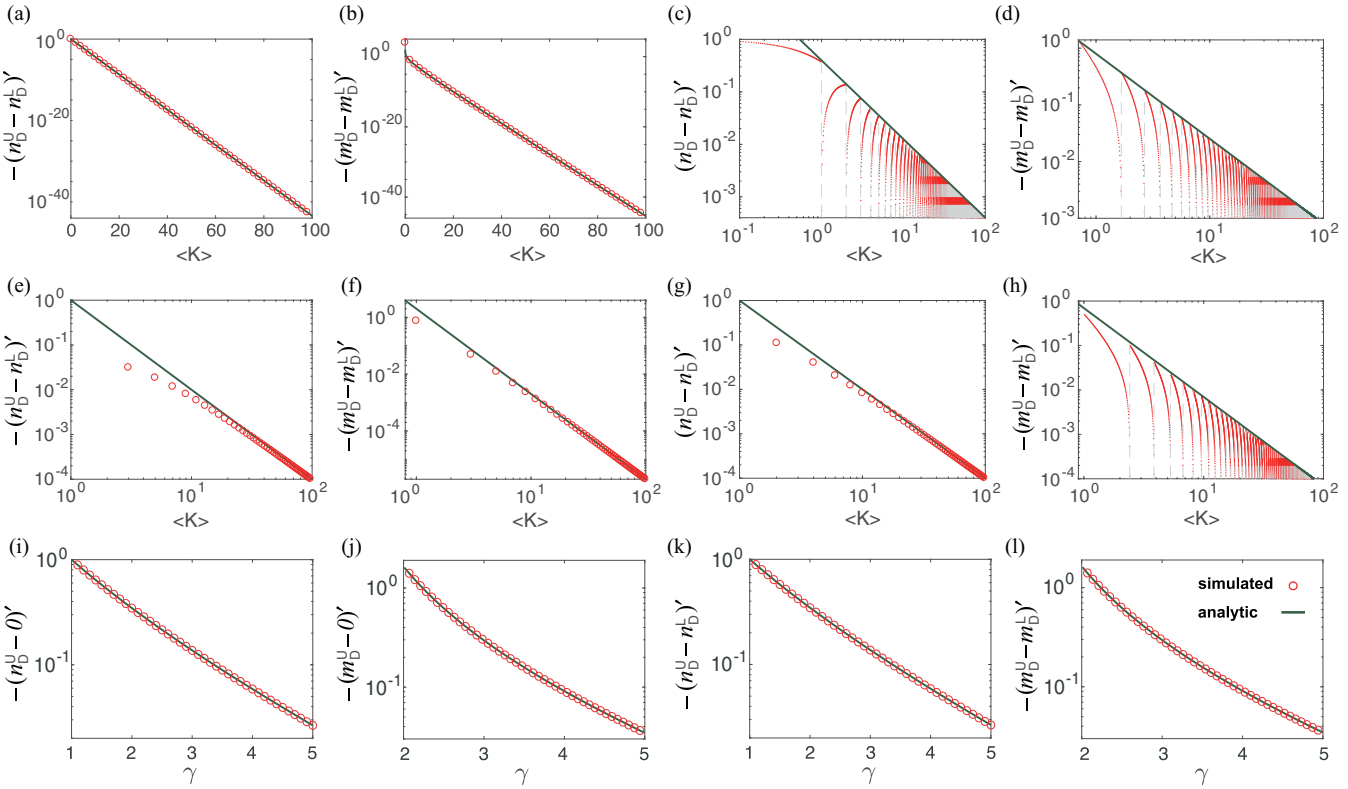

FIG. 3. Approach or separation speed. The approach or separation speed between the upper and lower limits in [(a)–(d)] ER networks and [(e)–(h)] EX networks as the function of the average degree $\langle k\rangle$ and in [(i)–(l)] SF networks as the function of the power-law exponent γ. The exponential cutoff parameter $\kappa \to \infty$ in (i)–(l). The speeds of model networks with unweighted switching matrices are shown in (a), (b), (e), (f), (i), and (j) and with structural switching matrices are shown in (c), (d), (g), (h), (k), and (l).

in ER networks with structural switching matrices and EX networks. In particular, as shown in Figs. 3(c), 3(d) and 3(h), the speed is discontinuous. This is due to the nonsmooth phenomenon in the upper limit of n_D and m_D in model networks. Note that Figs. 3(i)–3(l) only show the speed results of SF networks when $\kappa \to \infty$. The analytical results of the speed are presented in Appendix D, where simple and closed-form theoretical expectations are offered for all kinds of model networks.

V. CONTROLLABILITY LIMITS IN REAL NETWORKS

We use the tools developed above to study the edge controllability in real networks to determine the controllability limits. The upper and lower limits of n_D and m_D of different types of real networks are displayed in Table II. A notable finding is that there is a large gap between the upper and lower limits of n_D and m_D. This demonstrates the significant effect of the degree correlation on edge controllability of real networks.

Next we focus on the dependence of the controllability limits of real networks. As shown in Fig. 4, n_D and m_D of real networks with different $\langle k\rangle$ basically disperse in two regions, where the curves in two regions are the analytical results of the upper and lower limits of EX networks, respectively. The controllability limits of real networks with unweighted switching matrices disperse in two relatively small regions [see Figs. 4(a) and 4(c)] since their insensitivity to the network structure. By contrast, the affection of network structure on the controllability limits of real networks with structural switching matrices is much bigger, leading to much larger dispersion about the analytical prediction based on model network [see Figs. 4(b) and 4(d)]. Another prominent observation is that the lower limits n_D^L and m_D^L of real networks with structural switching matrices is much lower than that with unweighted switching matrices, which is in accordance with the results of model networks in Fig. 2. This indicates that the edge controllability of networks with structural switching matrices have a much higher potential to be optimized by perturbing the network structure.

In summary, instead of focusing on the degree distribution and the interaction strength, one has to take the degree correlation into account to offer a deeper and realistic understanding of the edge controllability in real networks, especially for the networks with structural switching matrices.

VI. CONCLUSION

We developed a framework to explore the effect of the correlation between in- and out-degrees on controlling edge dynamics in complex networks. Applying the framework to model and real networks, we find that the degree correlation plays an important role in edge controllability. To be specific, the existing results demonstrate that the controllability of nodal and edge dynamics is mainly determined by the degree distribution and the interaction strength [7,8,20,21]. However, our findings indicate that, to offer a better understanding

TABLE II. Controllability limits in real networks. For each network with unweighted switching matrices or structural switching matrices, we show its type, name, nodes number, edges number, and controllability limits.

					Unweighted switching matrices				Structural switching matrices			
Type	No.	Name	N	M	n_D^U	n_D^L	m_D^U	m_D^L	n_D^U	n_D^L	m_D^U	m_D^L
Regulatory	1	Ownership-USCorp [26]	8497	6726	0.159	0.061	1.000	0.799	0.159	0.028	0.875	0.738
	2	TRN-EC-2 [27]	423	578	0.274	0.182	0.879	0.799	0.274	0.071	0.879	0.545
	3	TRN-Yeast-1 [28]	4684	15451	0.064	0.057	0.985	0.981	0.064	0.025	0.985	0.802
	4	TRN-Yeast-2 [27]	688	1079	0.190	0.145	0.968	0.879	0.190	0.063	0.968	0.610
Trust	5	Prison inmate [29,30]	67	182	0.925	0.821	0.692	0.670	0.761	0.179	0.511	0.110
Food Web	6	St. Marks [31]	45	224	0.711	0.689	0.835	0.830	0.711	0.156	0.701	0.143
	7	Seagrass [32]	49	226	0.714	0.694	0.827	0.823	0.714	0.102	0.655	0.097
	8	Grassland [33]	88	137	0.341	0.330	0.620	0.613	0.341	0.148	0.620	0.314
	9	Ythan [33]	135	601	0.474	0.467	0.864	0.862	0.474	0.052	0.844	0.195
	10	Silwood [34]	154	370	0.214	0.208	0.897	0.895	0.214	0.084	0.897	0.508
	11	Little Rock [35]	183	2494	0.995	0.989	0.927	0.927	0.831	0.497	0.818	0.299
Electronic circuits	12	S208a [27]	122	189	0.549	0.541	0.413	0.407	0.549	0.311	0.413	0.201
	13	s420a [27]	252	399	0.560	0.556	0.416	0.414	0.560	0.325	0.416	0.206
	14	s838a [27]	512	819	0.564	0.563	0.418	0.416	0.565	0.332	0.418	0.208
Neuronal	15	C. elegans [36]	297	2359	0.949	0.859	0.881	0.880	0.923	0.081	0.639	0.069
Citation	16	Small World [37]	233	1988	0.309	0.300	0.451	0.450	0.309	0.047	0.869	0.469
	17	SciMet [37]	2729	10416	0.613	0.487	0.862	0.829	0.613	0.037	0.830	0.153
	18	Kohonen [38]	3772	12731	0.381	0.314	0.877	0.857	0.381	0.029	0.876	0.436
Internet	19	Political blogs [39]	1224	19090	0.870	0.769	0.953	0.945	0.870	0.165	0.908	0.163
	20	p2p-1 [40]	10876	39994	0.381	0.380	0.877	0.877	0.381	0.255	0.870	0.325
	21	p2p-2 [40]	8846	31839	0.387	0.374	0.883	0.879	0.387	0.265	0.878	0.352
	22	p2p-3 [40]	8717	31525	0.383	0.374	0.884	0.881	0.383	0.264	0.878	0.347
Organizational	23	Freeman-1 [41]	34	695	1.000	1.000	0.951	0.951	0.735	0.118	0.285	0.048
	24	Consulting [42]	46	879	1.000	1.000	0.950	0.950	0.848	0.109	0.369	0.079
Language	25	English words [43]	7381	46281	0.479	0.463	0.862	0.860	0.480	0.003	0.862	0.087
	26	French words [43]	8325	24295	0.333	0.290	0.736	0.721	0.333	0.009	0.736	0.092
Transportation	27	USair97 [44]	332	2126	0.762	0.602	0.894	0.869	0.762	0.030	0.861	0.045

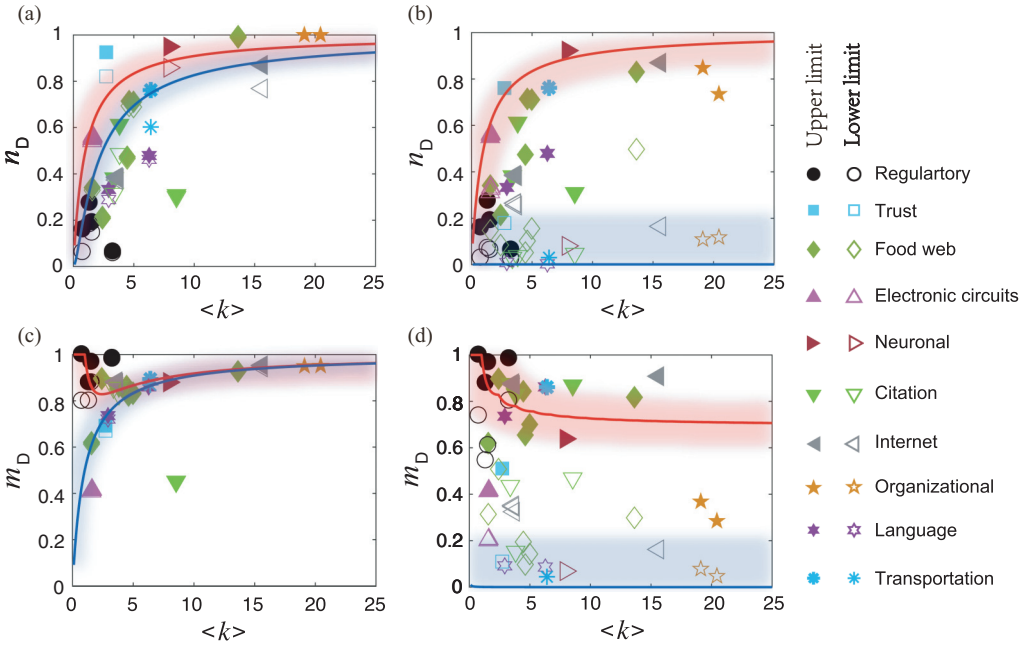

FIG. 4. Controllability limits in real networks. The upper and lower limits of driver nodes and driven edges in [(a) and (c)] real networks with unweighted switching matrices and in [(b) and (d)] real networks with structural switching matrices. The curves are analytical results of the controllability limits in EX networks.

of the edge controllability, it is imperative to consider the degree correlation. Furthermore, we explored the cause of the nonsmooth phenomenon in the controllability limits, and found the exponential and power-law scaling behaviors in the approach or separation speeds between the controllability limits.

Our results not only offer a new perspective on the role of network structure on edge controllability, but also raise several questions. Future research directions include how to optimize edge controllability by perturbing the network structure. The effect of degree correlation on the robustness, on the controllable subspace and target control, and on the energy consumption in control.

ACKNOWLEDGMENTS

S.-P.P. and F.H. are supported by NSFC under Grant No. 61573036. W.-X.W. was supported by NSFC under Grant No. 71631002.

APPENDIX A: MODEL NETWORK

A model network with N nodes is structured by given in- and out-degree distributions, including Poisson distribution, exponential distribution and power-law distribution. One can obtain a degree sequence by the given degree distribution, where the in- and out-degree sequences are denoted by $K_{\text{in}} = \{k_1^-, k_2^-, \ldots, k_N^-\}$ and $K_{\text{out}} = \{k_1^+, k_2^+, \ldots, k_N^+\}$, respectively. Note that N must be big enough to ensure the degree sequence is encoded completely by the degree distribution.

A directed network starts from N isolated nodes. Each node is assigned in-degree k_i^- and out-degree k_j^+ from in- and out-degree sequences, respectively. Two nodes u with $k_u^- > 0$ and node v with $k_v^+ > 0$ are randomly selected and connected with direction from node v to u. Then the in-degree of node u turns into $k_u^- - 1$ and the out-degree of node v turns into $k_v^+ - 1$. This process is repeated until all nodes satisfy the given in- and out-degrees. Note that the multiple edges in the generated network will be disposed by edges exchanging, i.e., turning edges e_{uv} and e_{kl} to edges e_{ul} and e_{kv} if there exist multiple edges e_{uv}, where $k \neq u$ and $l \neq v$.

APPENDIX B: ANALYTICAL RESULTS OF CONTROLLABILITY LIMIT

The analytical results of the controllability limits depend on the degree distribution. The in- and out-degrees of mode networks follow the same distribution, i.e., $P_k^{\text{in}} = P_k^{\text{out}} = P_k$.

We first give the analytical results of networks with unweighted switching matrices. The formulas for determining controllability limits in Table I enable us to directly give the analytical results. Specifically, the upper limit of n_D is

$$\begin{aligned} n_D^U &= \sum_{k=2}^{\infty} P_k + \min(P_0, P_1) \\ &= 1 - P_0 - P_1 + \min(P_0, P_1). \end{aligned} \tag{B1}$$

The lower limit of n_D is

$$\begin{aligned} n_D^L &= \sum_{k=2}^{\infty} P_k \\ &= 1 - P_0 - P_1. \end{aligned} \tag{B2}$$

The upper limit of m_D is

$$\begin{aligned} m_D^U &= \begin{cases} 1 \quad \text{if} \quad \sum_{k=1}^{\infty} P_k \leqslant P_0 \\ 1 - \frac{1}{\langle k \rangle}\left(\sum_{k=1}^{\infty} P_k - P_0\right) \quad \text{if} \quad \sum_{k=1}^{\infty} P_k > P_0 \end{cases} \\ &= \begin{cases} 1 \quad \text{if} \quad P_0 \geqslant 1/2 \\ 1 - \frac{1}{\langle k \rangle}(1 - 2P_0) \quad \text{if} \quad P_0 < 1/2 \end{cases}, \end{aligned} \tag{B3}$$

where the average degree is $\langle k \rangle = \langle k^+ \rangle = \langle k^- \rangle = M/N$. The lower limit of m_D is

$$\begin{aligned} m_D^L &= \frac{1}{\langle k \rangle}\left[\sum_{k=1}^{\infty} P_k (k-1)\right] \\ &= 1 - \frac{1}{\langle k \rangle}(1 - P_0). \end{aligned} \tag{B4}$$

Then we give the analytical results of networks with structural switching matrices. The upper limit of n_D is first considered. The exponent distribution of EX networks is monotone, i.e., $P_k > P_{k+1}$, where $k \in [0, k_{\max}]$. We assign each divergent node with $k_v^- = k_v^+ - 1$. The maximum number of those divergent nodes are determined by the number of nodes with $k_v^+ > 0$. Meanwhile, a node with $k_v^+ = 0$ must not be a divergent node. So the upper limit of n_D in EX networks is determined by the number of nodes with $k_v^+ > 0$, yielding

$$n_D^U = 1 - P_0. \tag{B5}$$

Evidenced by the same token, the upper limit of n_D in SF networks is also given by the above equation. Conversely, the poisson distribution of ER networks is unimodal and the degree of its peak is $k_{\text{peak}} = \lfloor \langle k \rangle \rfloor$, where $\lfloor \langle k \rangle \rfloor$ is the largest integer not greater than $\langle k \rangle$. The poisson distribution can be processed in two segments since it has a monotone increasing and a monotone decreasing at the left and right sides of its peak. So the upper limit of the number of driver nodes is $N_D^U = N_{(k_v^- < \lfloor \langle k \rangle \rfloor)} + N_{(k_v^+ > \lfloor \langle k \rangle \rfloor)}$. This leads to that the upper limit of n_D in ER networks is

$$n_D^U = 1 - P_{k_{\text{peak}}}. \tag{B6}$$

For the lower limit of n_D, we assign $k_i^- = k_i^+$ to each node to generate a connected network with no divergent nodes, yielding

$$n_D^L = \frac{1}{N}. \tag{B7}$$

To calculate the upper limit of m_D, we design a subtraction formula $\alpha - \beta$. Each time, the biggest degree $k_{\max}^+$ from the out-degree sequence and the smallest degree $k_{\min}^-$ from the in-degree sequence are selected to put into the set α and β, respectively. Meanwhile, the selected degrees are deleted from their degree sequences. Repeat the above steps until $k_{\max}^+ = k_{\min}^-$, we thus have the largest difference value between α and β. $\alpha - \beta$ is nothing but the upper limit of the number of driven edges. So the upper limit of m_D can be

described by

$$m_D^U = \frac{1}{\langle k\rangle}\left[\sum_{k=k_m+1}^{\infty} P_k k + \left(\frac{1}{2} - \sum_{k=k_m+1}^{\infty} P_k\right)k_m - \sum_{k=0}^{k_m-1} P_k k - \left(\frac{1}{2} - \sum_{k=0}^{k_m-1} P_k\right)k_m\right]$$
$$= \frac{1}{\langle k\rangle}\left[\sum_{k=0}^{k_m-1} P_k(k_m - k) + \sum_{k=k_m+1}^{\infty} P_k(k - k_m)\right], \tag{B8}$$

where k_m is the median of the ordered degree sequence in model networks. It satisfies

$$\sum_{k=0}^{k_m} P_k \geqslant \frac{1}{2} \quad \text{and} \quad \sum_{k=k_m}^{\infty} P_k \geqslant \frac{1}{2}. \tag{B9}$$

Note that, if $k_m = 0$, the upper limit of m_D is simplified to $m_D^U = \frac{1}{\langle k\rangle}\sum_{k=1}^{\infty} P_k k = 1$. For the lower limit of m_D, we assign $k_i^- = k_i^+$ to each node to generate a connected network with no divergent nodes, yielding

$$m_D^L = \frac{1}{M}. \tag{B10}$$

1. Poisson distributed network

For ER networks, both the in- and out-degrees follow the Poisson distribution, i.e.,$P(k_v^+ = k) = P(k_v^- = k) = \langle k\rangle^k e^{-\langle k\rangle}/k!$.

For ER networks with unweighted switching matrices, by substituting the Poisson distribution into Eq. (B1), we have

$$n_D^U = 1 - e^{-\langle k\rangle} - \langle k\rangle e^{-\langle k\rangle} + \min(e^{-\langle k\rangle}, \langle k\rangle e^{-\langle k\rangle})$$
$$= \begin{cases} 1 - e^{-\langle k\rangle} & \text{if } \langle k\rangle \leqslant 1 \\ 1 - \langle k\rangle e^{-\langle k\rangle} & \text{if } \langle k\rangle > 1 \end{cases}. \tag{B11}$$

Similarly, the lower limit of n_D is

$$n_D^L = 1 - e^{-\langle k\rangle} - \langle k\rangle e^{-\langle k\rangle}. \tag{B12}$$

By substituting the Poisson distribution into Eq. (B3), we have

$$m_D^U = \begin{cases} 1 & \text{if } \langle k\rangle \leqslant \ln 2 \\ 1 - \frac{1-2e^{-\langle k\rangle}}{\langle k\rangle} & \text{if } \langle k\rangle > \ln 2 \end{cases}. \tag{B13}$$

Similarly, the lower limit of m_D is

$$m_D^L = 1 - \frac{1}{\langle k\rangle}(1 - e^{-\langle k\rangle}). \tag{B14}$$

For ER networks with structural switching matrices, the upper limit of n_D is

$$n_D^U = 1 - P_{\lfloor\langle k\rangle\rfloor}$$
$$= 1 - \frac{e^{-\langle k\rangle}\langle k\rangle^{\lfloor\langle k\rangle\rfloor}}{\lfloor\langle k\rangle\rfloor!}. \tag{B15}$$

The lower limit of n_D is simply given by

$$n_D^L = \frac{1}{N}. \tag{B16}$$

The upper limit of m_D is

$$m_D^U = \frac{e^{-\langle k\rangle}}{\langle k\rangle}\left[\sum_{k=0}^{k_m-1}\frac{\langle k\rangle^k}{k!}(k_m - k) + \sum_{k=k_m+1}^{\infty}\frac{\langle k\rangle^k}{k!}(k - k_m)\right]$$
$$= \frac{1}{k_m!}[k_m! - k_m\Gamma(k_m, \langle k\rangle) - k_m(k_m - 1)\Gamma(k_m - 1, \langle k\rangle)]$$
$$+ \frac{k_m}{\langle k\rangle k_m!}[k_m\Gamma(k_m, \langle k\rangle) + \Gamma(k_m + 1, \langle k\rangle) - k_m!], \tag{B17}$$

where k_m satisfies

$$\frac{\Gamma(k_m + 1, \langle k\rangle)}{k_m!} \geqslant 1/2 \quad \text{and} \quad \frac{\Gamma(k_m, \langle k\rangle)}{(k_m - 1)!} \leqslant 1/2. \tag{B18}$$

The lower limit of m_D is simply given by

$$m_D^L = \frac{1}{N\langle k\rangle}. \tag{B19}$$

2. Exponentially distributed network

For EX networks, both the in- and out-degrees follow the exponential distribution, i.e., $P(k_v^+ = k) = P(k_v^- = k) = Ce^{-k/\kappa}$, where $C = 1 - e^{-1/\kappa}$ and $\kappa = 1/\log\frac{1+\langle k\rangle}{\langle k\rangle}$.

For EX networks with unweighted switching matrices, by substituting the exponential distribution into Eq. (B1), we have

$$n_D^U = 1 - C - Ce^{-1/\kappa} + \min(C, Ce^{-1/\kappa})$$
$$= \frac{\langle k\rangle}{\langle k\rangle + 1}. \tag{B20}$$

Similarly, the lower limit of n_D is

$$n_D^L = 1 - C - Ce^{-1/\kappa}$$
$$= \frac{\langle k\rangle^2}{(\langle k\rangle + 1)^2}. \tag{B21}$$

By substituting the exponential distribution into Eq. (B3), we have

$$m_D^U = \begin{cases} 1 & \text{if } C \geqslant 1/2 \\ 1 - \frac{1}{\langle k\rangle}(1 - 2C) & \text{if } C < 1/2 \end{cases}$$
$$= \begin{cases} 1 & \text{if } \langle k\rangle \leqslant 1 \\ \frac{\langle k\rangle^2+1}{\langle k\rangle^2+\langle k\rangle} & \text{if } \langle k\rangle > 1 \end{cases}. \tag{B22}$$

Similarly, the lower limit of m_D is

$$m_D^L = 1 - \frac{1}{\langle k\rangle}(1-C) = \frac{\langle k\rangle}{\langle k\rangle + 1}. \tag{B23}$$

For EX networks with structural switching matrices, the upper limit of n_D is

$$n_D^U = 1 - C = \frac{\langle k\rangle}{\langle k\rangle + 1}. \tag{B24}$$

The lower limit of n_D is simply given by

$$n_D^L = \frac{1}{N}. \tag{B25}$$

The upper limit of m_D is

$$m_D^U = \frac{C}{\langle k\rangle}\left[\sum_{k=0}^{k_m-1} e^{-k/\kappa}(k_m - k) + \sum_{k=k_m+1}^{\infty} e^{-k/\kappa}(k - k_m)\right] = 2\frac{\langle k\rangle^{k_m}}{(\langle k\rangle + 1)^{k_m}} + \frac{k_m}{\langle k\rangle} - 1, \tag{B26}$$

where k_m satisfies

$$\frac{\ln(1/2)}{\ln(\frac{\langle k\rangle}{\langle k\rangle+1})} \geqslant k_m \geqslant \frac{\ln(1/2)}{\ln(\frac{\langle k\rangle}{\langle k\rangle+1})} - 1. \tag{B27}$$

The lower limit of m_D is simply given by

$$m_D^L = \frac{1}{N\langle k\rangle}. \tag{B28}$$

3. Power-law distributed network

For SF networks, both in- and out-degrees follow the same power-law distribution with power-law exponent γ and an exponential cutoff, i.e., $P(k_v^+ = k) = P(k_v^- = k) = Ck^{-\gamma}e^{-k/\kappa}$, where $C = 1/\mathrm{Li}_\gamma(e^{-1/\kappa})$, $\langle k\rangle = C\mathrm{Li}_{\gamma-1}(e^{-1/\kappa})$, and $\mathrm{Li}_s(z)$ is the polylogarithm function. Note that $P_0 = 0$ in SF networks.

For SF networks with unweighted switching matrices, there is no nodes with $k_v^+ = 0$ or $k_v^- = 0$ in networks. So the number of driver nodes in the upper limit is always the same as that in the lower limit. Thus, the expected fraction of driver nodes in both upper and lower limits is

$$n_D = 1 - \frac{e^{-1/\kappa}}{\mathrm{Li}_\gamma(e^{-1/\kappa})}. \tag{B29}$$

When $\kappa \to \infty$, the exponential cutoff vanishes and the polylogarithm function reduces to the Riemann ζ function $\zeta(s)$. So the function of driver nodes in both upper and lower limits is simplified as $n_D = 1 - 1/\zeta(\gamma)$. For the same reason, the expected fraction of driven edges in both upper and lower limits is

$$m_D = 1 - \frac{\mathrm{Li}_\gamma(e^{-1/\kappa})}{\mathrm{Li}_{\gamma-1}(e^{-1/\kappa})}. \tag{B30}$$

When $\kappa \to \infty$, it is simplified as $m_D = 1 - \zeta(\gamma)/\zeta(\gamma-1)$.

For SF networks with structural switching matrices, the upper limit of n_D is

$$n_D^U = 1 - P_1 = 1 - \frac{e^{-1/\kappa}}{\mathrm{Li}_\gamma(e^{-1/\kappa})}. \tag{B31}$$

When $\kappa \to \infty$, it is simplified as $n_D^U = 1 - 1/\zeta(\gamma)$. The lower limit of n_D is

$$n_D^L = \frac{1}{N}. \tag{B32}$$

The upper limit of m_D is

$$\begin{aligned} m_D^U &= \frac{C}{\langle k\rangle}\left[\sum_{k=0}^{k_m-1} k^{-\gamma}e^{-k/\kappa}(k_m - k) + \sum_{k=k_m+1}^{\infty} k^{-\gamma}e^{-k/\kappa}(k - k_m)\right] \\ &= \frac{e^{-(k_m+1)/\kappa}}{\mathrm{Li}_{\gamma-1}(e^{-1/\kappa})}[\Phi(e^{-1/\kappa}, \gamma-1, k_m+1) - k_m\Phi(e^{-1/\kappa}, \gamma, k_m+1)] - 1 \\ &\quad + \frac{e^{-k_m/\kappa}}{\mathrm{Li}_{\gamma-1}(e^{-1/\kappa})}[\Phi(e^{-1/\kappa}, \gamma-1, k_m) - k_m\Phi(e^{-1/\kappa}, \gamma, k_m)] + \frac{k_m\mathrm{Li}_\gamma(e^{-1/\kappa})}{\mathrm{Li}_{\gamma-1}(e^{-1/\kappa})}, \end{aligned} \tag{B33}$$

where $\Phi(z, s, a)$ is the Lerch transcendent function and k_m satisfies

$$\frac{e^{-(k_m+1)/\kappa}\Phi(e^{-1/\kappa}, \gamma, k_m+1)}{\mathrm{Li}_\gamma(e^{-1/\kappa})} \leqslant \frac{1}{2} \quad \text{and} \quad \frac{e^{-k_m/\kappa}\Phi(e^{-1/\kappa}, \gamma, k_m)}{\mathrm{Li}_\gamma(e^{-1/\kappa})} \geqslant \frac{1}{2}. \tag{B34}$$

When $\kappa \to \infty$, it is simplified as

$$m_D^U = \frac{1}{\zeta(\gamma-1)}[\zeta(\gamma-1, k_m) + \zeta(\gamma-1, k_m+1)] - \frac{k_m}{\zeta(\gamma-1)}[\zeta(\gamma, k_m) + \zeta(\gamma, k_m+1) - \zeta(\gamma)] - 1, \tag{B35}$$

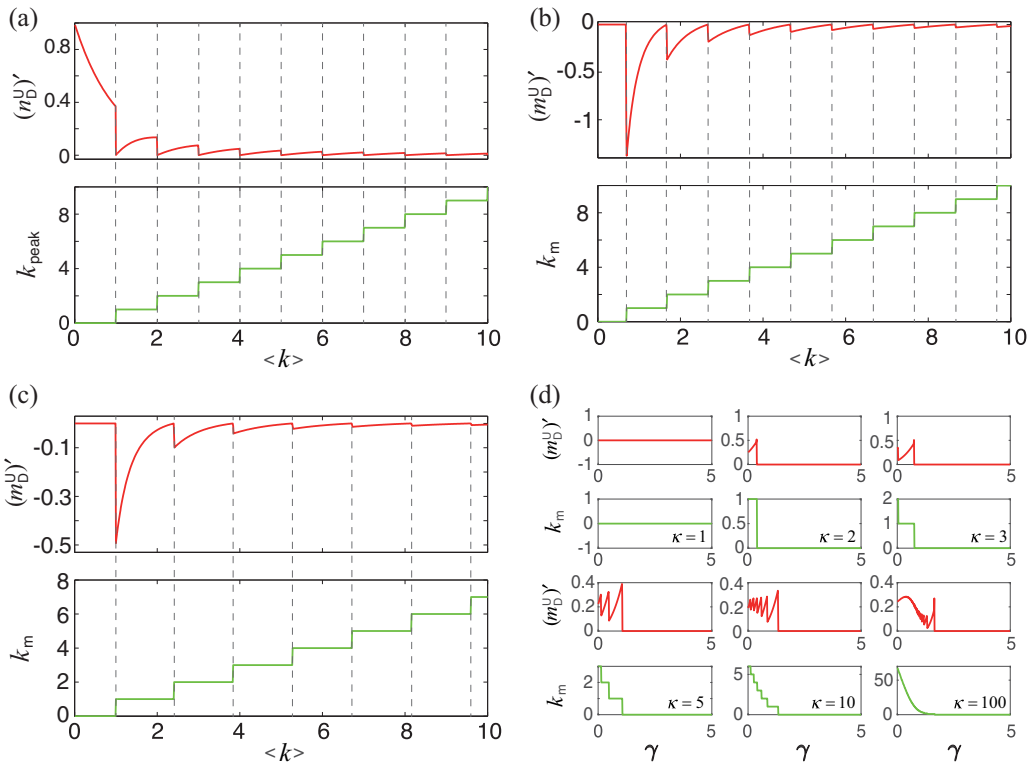

FIG. 5. Nonsmooth phenomenon. (a) The correspondence between $(n_D^U)'$ and k_{peak} in ER networks. [(b)–(d)] The correspondence between $(m_D^U)'$ and k_m in ER, EX, and SF networks.

where $\zeta(s, a)$ is the Hurwitz ζ function and k_m satisfies

$$\frac{\zeta(\gamma, k_m + 1)}{\zeta(\gamma)} \leqslant \frac{1}{2} \quad \text{and} \quad \frac{\zeta(\gamma, k_m)}{\zeta(\gamma)} \geqslant \frac{1}{2}. \tag{B36}$$

The lower limit of m_D is

$$m_D^L = \frac{\text{Li}_\gamma(e^{-1/\kappa})}{N\text{Li}_{\gamma-1}(e^{-1/\kappa})}. \tag{B37}$$

When $\kappa \to \infty$, it is simplified as $m_D^L = \zeta(\gamma)/[N\zeta(\gamma - 1)]$.

APPENDIX C: NONSMOOTH PHENOMENON

A nonsmooth phenomenon exists in n_D^U of ER networks, and m_D^U of ER, EX, and SF networks. Figure 5(a) shows the correspondence between $(n_D^U)'$ and k_{peak} in ER networks. The simulation results indicate that the nonsmooth phenomenon in n_D^U of ER networks is caused by k_{peak}. Evidenced by the same token, as shown in Figs. 5(b)–5(d), the nonsmooth phenomenon in m_D^U is caused by k_m. The analytical results are presented in Appendix D.

APPENDIX D: ANALYSIS RESULTS OF SPEED

1. Poisson distributed network

For ER network with unweighted switching matrices, when $\langle k \rangle > 1$, the approach speed between n_D^U and n_D^L is

$$\left(n_D^U - n_D^L\right)' = -e^{-\langle k \rangle}. \tag{D1}$$

When $\langle k \rangle > \ln 2$, the approach speed between m_D^U and m_D^L is

$$\begin{aligned}\left(m_D^U - m_D^L\right)' &= -\frac{e^{-\langle k \rangle}}{\langle k \rangle^2} - \frac{e^{-\langle k \rangle}}{\langle k \rangle} \\ &\approx -\frac{1}{\langle k \rangle} e^{-\langle k \rangle}.\end{aligned} \tag{D2}$$

For ER networks with structural switching matrices, we calculate the speeds by neglecting the lower controllability limit since $n_D^L = 1/N$ and $m_D^L = 1/M$. The nonsmooth phenomenon is presented in the upper limit of n_D of ER networks. According to Eq. (B15), the nonsmooth phenomenon stems from $P_{\text{peak}} = \lfloor \langle k \rangle \rfloor$. The parameter $\lfloor \langle k \rangle \rfloor$ changes from $\langle k \rangle - 1$ to $\langle k \rangle$ at the jump point. Thus, when $\lfloor \langle k \rangle \rfloor = \langle k \rangle - 1$, the separation speed between n_D^U and n_D^L is given by

$$\begin{aligned}\left(n_D^U - n_D^L\right)' &= e^{-\langle k \rangle}\left(\frac{\langle k \rangle^{\langle k \rangle - 1}}{(\langle k \rangle - 1)!} - \frac{\langle k \rangle^{\langle k \rangle - 2}}{(\langle k \rangle - 2)!}\right) \\ &= \frac{1}{\sqrt{2\pi}} \langle k \rangle^{-1.5}.\end{aligned} \tag{D3}$$

When $\lfloor \langle k \rangle \rfloor = \langle k \rangle$, the separation speed is

$$\begin{aligned}\left(n_D^U - n_D^L\right)' &= e^{-\langle k \rangle}\left[\frac{\langle k \rangle^{\langle k \rangle}}{(\langle k \rangle)!} - \frac{\langle k \rangle^{\langle k \rangle - 1}}{(\langle k \rangle - 1)!}\right]. \\ &= 0.\end{aligned} \tag{D4}$$

The approach speed between m_D^U and m_D^L is

$$\begin{aligned}\left(m_D^U - m_D^L\right)' &= \frac{\langle k\rangle^{k_m-1}e^{-\langle k\rangle}}{(k_m-1)!} + \frac{\langle k\rangle^{k_m-2}e^{-\langle k\rangle}}{(k_m-2)!} + \left[\frac{-\langle k\rangle^{k_m-1}e^{-\langle k\rangle}}{(k_m-1)!} + \frac{-\langle k\rangle^{k_m}e^{-\langle k\rangle}}{k_m!}\right]\frac{k_m}{\langle k\rangle} \\ &\quad - \left[\frac{\Gamma(k_m,\langle k\rangle)}{(k_m-1)!} + \frac{\Gamma(k_m+1,\langle k\rangle)}{k_m!} - 1\right]\frac{k_m}{\langle k\rangle^2} \\ &= -\frac{e^{-\langle k\rangle}\langle k\rangle^{k_m-2}}{(k_m-1)!} - \left[\frac{\Gamma(k_m,\langle k\rangle)}{(k_m-1)!} + \frac{\Gamma(k_m+1,\langle k\rangle)}{k_m!} - 1\right]\frac{k_m}{\langle k\rangle^2}. \end{aligned} \tag{D5}$$

Note that the nonsmooth phenomenon is presented in the upper limit of m_D. According to Eq. (B17), the nonsmooth phenomenon stems from k_m. The parameter k_m is determined by Eq. (B18). Thus, when $\Gamma(k_m,\langle k\rangle)/(k_m-1)! = 1/2$, the approach speed is

$$\begin{aligned}\left(m_D^U - m_D^L\right)' &= -\frac{e^{-\langle k\rangle}\langle k\rangle^{\langle k\rangle-1}}{\sqrt{2\pi\langle k\rangle}(\langle k\rangle/e)^{\langle k\rangle}} - \left[-\frac{1}{2} + \frac{\langle k\rangle\Gamma(\langle k\rangle,\langle k\rangle) + \langle k\rangle^{\langle k\rangle}e^{-\langle k\rangle}}{\sqrt{2\pi\langle k\rangle}(\langle k\rangle/e)^{\langle k\rangle}}\right]\langle k\rangle^{-1} \\ &= -\frac{2}{\sqrt{2\pi}}\langle k\rangle^{-1.5}. \end{aligned} \tag{D6}$$

When $\Gamma(k_m+1,\langle k\rangle)/k_m! = 1/2$, the approach speed is

$$\begin{aligned}\left(m_D^U - m_D^L\right)' &= -\frac{e^{-\langle k\rangle}\langle k\rangle^{\langle k\rangle-1}}{\sqrt{2\pi\langle k\rangle}(\langle k\rangle/e)^{\langle k\rangle}} - \left[-\frac{1}{2} + \frac{\Gamma(\langle k\rangle+1,\langle k\rangle) - \langle k\rangle^{\langle k\rangle}e^{-\langle k\rangle}}{\sqrt{2\pi\langle k\rangle}(\langle k\rangle/e)^{\langle k\rangle}}\right]\langle k\rangle^{-1} \\ &= 0. \end{aligned} \tag{D7}$$

2. Exponentially distributed network

For EX networks with unweighted switching matrices, the approach speed between n_D^U and n_D^L is

$$\begin{aligned}\left(n_D^U - n_D^L\right)' &= \frac{1-\langle k\rangle}{(1+\langle k\rangle)^3} \\ &\approx -\langle k\rangle^{-2}. \end{aligned} \tag{D8}$$

When $\langle k\rangle > 1$, the approach speed between m_D^U and m_D^L is

$$\begin{aligned}\left(m_D^U - m_D^L\right)' &= -\frac{2\langle k\rangle+1}{(\langle k\rangle^2+\langle k\rangle)^2} \\ &\approx -2\langle k\rangle^{-3}. \end{aligned} \tag{D9}$$

For EX networks with structural switching matrices, we calculate the speeds by neglecting the lower controllability limit since $n_D^L = 1/N$ and $m_D^L = 1/M$. So the separation speed between n_D^U and n_D^L is

$$\left(n_D^U - n_D^L\right)' = (\langle k\rangle+1)^{-2} \approx \langle k\rangle^{-2}. \tag{D10}$$

The approach speed between m_D^U and m_D^L is

$$\left(m_D^U - m_D^L\right)' = 2k_m\left(\frac{\langle k\rangle}{\langle k\rangle+1}\right)^{k_m-1}(\langle k\rangle+1)^{-2} - k_m\langle k\rangle^{-2}. \tag{D11}$$

Note that the nonsmooth phenomenon is presented in the upper limit of m_D. According to Eq. (B26), the nonsmooth phenomenon stems from k_m. The parameter k_m is determined by Eq. (B27). Thus, when $k_m = \ln(1/2)/\ln(\langle k\rangle/(\langle k\rangle+1))$, the approach speed is

$$\begin{aligned}\left(m_D^U - m_D^L\right)' &= 2\frac{\ln\frac{1}{2}}{\ln\frac{\langle k\rangle}{\langle k\rangle+1}}\frac{1/2}{\langle k\rangle/(\langle k\rangle+1)}(\langle k\rangle+1)^{-2} - \frac{\ln\frac{1}{2}}{\ln\frac{\langle k\rangle}{\langle k\rangle+1}}\langle k\rangle^{-2} \\ &= \ln\tfrac{1}{2}\langle k\rangle^{-2}. \end{aligned} \tag{D12}$$

When $k_m = \ln(1/2)/\ln(\langle k\rangle/[\langle k\rangle+1)] - 1$, the approach speed is

$$\begin{aligned}\left(m_D^U - m_D^L\right)' &= \left(\frac{\ln\frac{1}{2}}{\ln\frac{\langle k\rangle}{\langle k\rangle+1}} - 1\right)\left[\left(\frac{\langle k\rangle}{\langle k\rangle+1}\right)^{-2}(\langle k\rangle+1)^{-2} - \langle k\rangle^{-2}\right] \\ &= 0. \end{aligned} \tag{D13}$$

3. Power-law distributed network

For SF networks with unweighted switching matrices, the number of driver nodes and driven edges in the upper limit is always the same as that in the lower limit. We calculate the approach speed between the controllability limit and the zero value. When $\kappa \to \infty$, the approach speed between n_D and 0 is

$$(n_D - 0)' = \frac{\zeta'(\gamma)}{\zeta(\gamma)^2}. \tag{D14}$$

When $\kappa \to \infty$, the approach speed between m_D and 0 is

$$(m_D - 0)' = \frac{1}{\zeta(\gamma-1)^2}[\zeta(\gamma)\zeta'(\gamma-1) - \zeta'(\gamma)\zeta(\gamma-1)]. \tag{D15}$$

For SF networks with structural switching matrices, we calculate the speeds by neglecting the lower controllability limit since $n_D^L = 1/N$ and $m_D^L = 1/M$. When $\kappa \to \infty$, the separation speed between n_D^U and n_D^L is

$$\left(n_D^U - n_D^L\right)' = \frac{\zeta'(\gamma)}{\zeta(\gamma)^2}. \tag{D16}$$

When $\kappa \to \infty$ and $\gamma > 2$, median $k_m \equiv 1$ and $m_D^U = 1 - \zeta(\gamma)/\zeta(\gamma-1)$. So the approach speed between m_D^U and m_D^L is

$$\left(m_D^U - m_D^L\right)' = \frac{1}{\zeta(\gamma-1)^2}[\zeta(\gamma)\zeta'(\gamma-1) - \zeta'(\gamma)\zeta(\gamma-1)]. \tag{D17}$$

[1] S. Boccaletti, V. Latora, Y. Moreno, M. Chavez, and D.-U. Hwang, Complex networks: Structure and dynamics, Phys. Rep. **424**, 175 (2006).

[2] M. E. J. Newman, *Networks: An Introduction* (Oxford University Press, Oxford, 2010).

[3] A.-L. Barabási, *Network Science* (Cambridge University Press, Cambridge, 2016).

[4] F. Sorrentino, M. diBernardo, F. Garofalo, and G. Chen, Controllability of complex networks via pinning, Phys. Rev. E **75**, 046103 (2007).

[5] B. Liu, T. Chu, L. Wang, and G. Xie, Controllability of a leader-follower dynamic network with switching topology, IEEE Trans. Automat. Contr. **53**, 1009 (2008).

[6] W. Yu, G. Chen, and J. Lü, On pinning synchronization of complex dynamical networks, Automatica **45**, 429 (2009).

[7] Y.-Y. Liu, J.-J. Slotine, and A.-L. Barabási, Controllability of complex networks, Nature **473**, 167 (2011).

[8] Z. Yuan, C. Zhao, W.-X. Wang, and Y.-C. Lai, Exact controllability of complex networks, Nat. Commun. **4**, 2447 (2013).

[9] W.-X. Wang, X. Ni, Y.-C. Lai, and C. Grebogi, Optimizing controllability of complex networks by minimum structural perturbations, Phys. Rev. E **85**, 026115 (2012).

[10] S. P. Cornelius, W. L. Kath, and A. E. Motter, Realistic control of network dynamics, Nat. Commun. **4**, 1942 (2013).

[11] M. Pósfai, Y. Y. Liu, J. J. Slotine, and A. L. Barabási, Effect of correlations on network controllability, Sci. Rep. **3**, 1067 (2013).

[12] T. Jia, Y. Y. Liu, E. Csóka, M. Pósfai, J. J. Slotine, and A. L. Barabási, Emergence of bimodality in controlling complex networks, Nat. Commun. **4**, 2002 (2013).

[13] M. Galbiati, D. Delpini, and S. Battiston, The power to control, Nat. Phys. **9**, 126 (2013).

[14] J. Ruths, and D. Ruths, Control profiles of complex networks, Science **343**, 1373 (2014).

[15] J. Gao, Y. Y. Liu, R. M. Dsouza, and A. L. Barabási, Target control of complex networks, Nat. Commun. **5**, 5415 (2014).

[16] G. Yan, G. Tsekenis, B. Barzel, J. J. Slotine, Y. Y. Liu, and A. L. Barabási, Spectrum of controlling and observing complex networks, Nat. Phys. **11**, 779 (2015).

[17] S. P. Pang, F. Hao, and W. X. Wang, Robustness of controlling edge dynamics in complex networks against node failure, Phys. Rev. E **94**, 052310 (2016).

[18] Y. Z. Sun, S. Y. Leng, Y. C. Lai, C. Grebogi, and W. Lin, Closed-Loop Control of Complex Networks: A Trade-Off Between Time and Energy, Phys. Rev. Lett. **119**, 198301 (2017).

[19] Y. Y. Liu, and A. L. Barabási, Control principles of complex systems, Rev. Mod. Phys. **88**, 035006 (2016).

[20] T. Nepusz, and T. Vicsek, Controlling edge dynamics in complex networks, Nat. Phys. **8**, 568 (2012).

[21] S. P. Pang, W. X. Wang, F. Hao, and Y. C. Lai, Universal framework for edge controllability of complex networks, Sci. Rep. **7**, 4224 (2017).

[22] N. Schwartz, R. Cohen, D. Ben-Avraham, A. L. Barabási, and S. Havlin, Percolation in directed scale-free networks, Phys. Rev. E **66**, 015104(R) (2002).

[23] G. Bianconi, N. Gulbahce, and A. E. Motter, Local Structure of Directed Networks, Phys. Rev. Lett. **100**, 118701 (2008).

[24] P. Erdős and A. Rényi, On the evolution of random graphs, Publ. Math. Inst. Hung. Acad. Sci. **5**, 17 (1960).

[25] A.-L. Barabási, and R. Albert, Emergence of scaling in random networks, Science **286**, 509 (1999).

[26] K. Norlen, G. Lucas, M. Gebbie, and J. Chuang, EVA: Extraction, visualization and analysis of the telecommunications and media ownership network, in *Proceedings of the International Telecommunications Society 14th Biennial Conference (ITS'02)* (Elsevier, South Korea, 2002).

[27] R. Milo, S. Shen-Orr, S. Itzkovitz, N. Kashtan, D. Chklovskii, and U. Alon, Network motifs: Simple building blocks of complex networks, Science **298**, 824 (2002).

[28] S. Balaji, M. Babu, L. Iyer, N. Kashtan, and L. Aravind, Comprehensive analysis of combinatorial regulation using the transcriptional regulatory network of yeast, J. Mol. Biol. **360**, 213 (2006).

[29] R. Milo, S. Itzkovitz, N. Kashtan, R. Levitt, S. Shen-Orr, I. Ayzenshtat, M. Sheffer, and M. Sheffer, Superfamilies of evolved and designed networks, Science **303**, 1538 (2004).

[30] M. A. J. Van Duijn, E. P. H. Zeggelink, M. Huisman, F. N. Stokman, and F. W. Wasseur, Evolution of sociology freshmen into a friendship network, J. Math. Sociol. **27**, 153 (2003).

[31] D. Baird, J. Luczkovich, and R. R. Christian, Assessment of spatial and temporal variability in ecosystem attributes of the St Marks National Wildlife Refuge, Apalachee Bay, Florida. Est. Coast. Shelf Sci. **47**, 329 (1998).

[32] R. R. Christian and J. J. Luczkovich, Organizing and understanding a winter's seagrass food web network through effective trophic levels, Ecol. Model. **117**, 99 (1999).

[33] J. A. Dunne, R. J. Williams, and N. D. Martinez, Food-web structure and network theory: The role of connectance and size, Proc. Natl. Acad. Sci. USA **99**, 12917 (2002).

[34] J. Memmott, N. D. Martinez, and J. E. Cohen, Predators, parasitoids and pathogens: species richness, trophic generality and body sizes in a natural food web, J. Animal Ecology **69**(1), 1 (2000).

[35] N. D. Martinez, Artifacts or attributes? Effects of resolution on the Little Rock Lake food web, Ecol. Monogr. **61**, 367 (1991).

[36] D. J. Watts and S. H. Strogatz, Collective dynamics of 'small-world' networks, Nature **393**, 440 (1998).

[37] http://vlado.fmf.uni-lj.si/pub/networks/data/cite/default.htm.

[38] http://www.cise.ufl.edu/research/sparse/matrices/Pajek/Kohonen.html.

[39] L. A. Adamic and N. Glance, The political blogosphere and the 2004 US election: Divided they blog, in *Proceedings of the 3rd International Workshop on Link Discovery*, LinkKDD '05 (ACM, New York, 2005), pp. 36–43.

[40] J. Leskovec, J. Kleinberg, and C. Faloutsos, Graph evolution: Densification and shrinking diameters, ACM Trans. Knowl. Discov. Data **1**, 2 (2007).

[41] S. Wasserman and K. Faust, *Social Network Analysis: Methods and Applications* (Cambridge University Press, Cambridge, 1994).

[42] R. L. Cross and A. Parker, *The Hidden Power of Social Networks: Understanding How Work Really Gets Done in Organizations* (Harvard Business Review Press, Cambrdidge, MA, 2004).

[43] http://www.clairlib.org/index.php/Corpora.

[44] http://vlado.fmf.uni-lj.si/pub/networks/data/mix/USAir97.net.